Two-Dimensional Penning Ionization Electron Spectroscopy of Monobromothiophenes: Orbital Reactivity and Anisotropic Interaction with He*(2^3S) Metastable Atom

Shan Xi Tian, Naoki Kishimoto, and Koichi Ohno*

Department of Chemistry, Graduate School of Science, Tohoku University, Aramaki, Aoba-ku, Sendai 980-8578, Japan

Received: March 27, 2002; In Final Form: June 18, 2002

Penning ionization of 2-bromothiophene and 3-bromothiophene by collision with He*(2^3S) metastable atoms is studied using two-dimensional (collision-energy and electron-energy- resolved) Penning ionization electron spectroscopy. Some satellite bands correlated with ionic states of π orbitals are observed in Penning ionization electron spectra. Collision energy dependence of partial ionization cross sections indicates that attractive interactions of the He* out-of-plane approach respective to the thiophenyl ring including bromine atom are much stronger than those of the in-plane approach. Substitution of the bromine atom holds the sequence of magnitude of attractive interaction for the out-of-plane approach $\pi_2 > \pi_3 > n_S$ which was previously observed for thiophene. Different substitution sites lead to the change of Penning ionization activity of the in-plane lone pair orbital of the bromine atom, which is interpreted as a result of intramolecular orbital interactions.

I. Introduction

Two-dimensional (collision-energy and electron-energy-resolved) Penning ionization electron spectroscopy can provide us with information of the anisotropic interactions around target molecules.[1−7] The theoretical approach for this experimental technique is based upon the electron exchange model of the Penning ionization process[8] and molecular local orbital approximations.[9−12] Namely, the former exhibits that the mutual overlap of related orbitals in the electron exchange (e.g., the 2s orbital of a metastable atom He*(2^3S) and a certain outer valence orbital of a target molecule) plays a central role in Penning ionization; the latter means that electron densities of a molecular orbital (MO) are more or less localized on a particular part of the target molecule. For a two-dimensional Penning ionization electron spectrum (2D-PIES), an ionization band (corresponding to one ionic state or more) in the normalized collision-energy-resolved Penning ionization electron spectra (CERPIES) obtained from the 2D-PIES usually becomes stronger or weaker as the collision energy (E_c) increases. Accordingly, partial ionization cross sections can be plotted against the E_c values, and they exhibit negative, flat, or positive slopes. This collision energy dependence of partial ionization cross sections (CED-PICS) reflects the dynamics of Penning ionization for an MO, further exhibiting anisotropic interactions between the metastable atom (e.g., the He*(2^3S) atom) and the target molecule. Moreover, experimental branching ratios of ionic states in a collision-energy-averaged PIES can be roughly simulated by the exterior electron density (EED) of the target MO exposed outside the molecular surface.[9−12] An ionic state of the MO having more exterior electrons should exhibit a high band in PIES. Therefore, PIES also provides us with information on the electron distribution of the target MOs exposed outside the boundary surface of collision, whereas almost full-spaced electron distributions of MOs can be investigated by electron momentum spectroscopy.[13]

Obviously, cross sections of the Penning ionization depend not only on the electron density distribution of the target MO but also on the characteristics of interactions between the colliding particles. Furthermore, the collision boundary surface should depend on the collision energy. If an ionization reaction is mostly governed by the attractive interaction, the ionization cross section should be enhanced at lower collision energies, because the slower He*(2^3S) atom can approach the attractive region effectively. On the contrary, the cross section should be enhanced at higher energies if the repulsive interaction governs the ionization, because the faster He*(2^3S) atoms can approach the reactive region more effectively.

Among a number of 2D-PIES investigations on various molecules,[3−7] the interactions for the localized MOs have been studied very well because those attractive or repulsive interactions localized in some specific regions were distinctly anisotropic. However, the electron density distribution of an MO is not always localized, which may be due to intramolecular through-space or through-bond interaction and hyperconjugation of MOs.[14] We should take insights into molecular electronic structure and reaction dynamics for the target molecules having delocalized MOs, through comparative 2D-PIES studies on some similar target molecules including their substituted derivatives. Recently, a series of studies on substituted benzenes (aniline, phenol, and thiophenol),[3] monohalogenobenzenes,[4] and dihalogenobenzenes[5,6] have been reported. It is interesting how a lone pair orbital (n) interacts with a π orbital and how such interactions reflect on the slopes of CEDPICS for the related bands. Unfortunately, a direct comparison is unattainable for the dihalogenobenzenes because the bands in their PIES are seriously overlapped.[6] As for monohalogenobenzenes, there is no dependence on the substitution sites.[4] Monobromothiophenes are suitable for studying both $n-\pi$ orbital interaction and substitution site effect, because of the well-resolved bands in the higher electron kinetic-energy (E_e) region of the electron spectra and a lower molecular symmetry (C_s).[15−17] 2-bromothiophene (2BT) and 3-bromothiophene (3BT) are investigated by

* To whom correspondence should be addressed.

10.1021/jp020825q CCC: $22.00
Published on Web 08/07/2002

2D Penning ionization electron spectroscopy in this work, the relative reactivity of orbitals with the He*(2^3S) atom is discussed on the basis of model calculations of interaction potential energies and in comparison with the results of monobromobenzene[4] and thiophene.[7] Moreover, thiophene is used in major pharmaceutical application, veterinary drugs, dyes, and polymers, and the major use of 2BT is an anti-tussive preparation. Continuous interest in these molecules having medical and biological usages is also of this project.

II. Experimental Section

Details of the experimental apparatus have been reported elsewhere.[7,18−20] Metastable atoms of He*(2^1S, 2^3S) were produced by a discharged nozzle source with a tantalum hollow cathode. The He*(2^1S) component was quenched by a water-cooled helium discharge lamp. He I resonance photons (584 Å, 21.22 eV) produced by a discharge in pure helium gas were used to obtain UPS. The kinetic energies of the electrons ejected in Penning ionization or photo ionization were determined by a hemispherical electrostatic deflection type analyzer using an electron collection angle 90° to the incident He*(2^3S) beam axis or He I light beam axis. The energy resolution of the electron analyzer was estimated to be 80 meV from the full width at half-maximum (fwhm) of the $Ar^+(^2P_{3/2})$ peak in the He I UPS for the energy-higher-resolution PIES and UPS measurements of the samples; for the CEDPICS measurements, the resolution was lowered to 250 meV in order to obtain higher electron counting rates. The transmission efficiency curves of the electron energy analyzer for both of these two modes were determined by comparing our UPS data of some molecules with those obtained by Gardner and Samson[21] and Kimura et al.[22] The calibration of the electron energy scale was made with reference to the lowest ionic state of molecule nitrogen mixed with the sample molecule in He I UPS (E_e = 5.639 eV) and He*(2^3S) PIES (E_e = 4.292 eV) including a peak energy shift of 50 meV and the difference between the metastable excitation energy and the lowest IP.

For the collision-energy-resolved measurements of Penning ionization, the metastable He*(2^3S) beam was modulated by a pseudorandom chopper rotating at ca. 370 Hz and then introduced into a reaction cell located at 504 mm downstream from the chopper disk. Time dependent electron signals for each E_e were recorded with scanning electron energies of a 40 meV step, and the dwell time for the TOF measurements was 3 μs. The two-dimensional data as functions of E_e and time t were stored in a 2MB RAM. Two-dimensional spectra $I_e(E_e,t_{TOF})$, functions of E_e and TOF, can lead to $I_e(E_e,v_{He^*})$, functions of E_e and the velocity of He* (v_{He^*}), and then to the 2D Penning ionization cross-section $\sigma(E_e,v_r)$ using the equations

$$\sigma(E_e,v_r) = c\{I_e(E_e,v_{He^*})/I_{He^*}(v_{He^*})\}(v_{He^*}/v_r) \quad (1)$$

$$v_r = [v_{He^*}{}^2 + 3kT/M]^{1/2} \quad (2)$$

where c is a constant, v_r is the relative velocity averaged over the velocity of the target molecule, k is the Boltzmann constant, and T and M are the gas temperature and mass of the target molecule, respectively. The velocity distribution $I_{He^*}(v_{He^*})$ of the He* beam was determined by monitoring secondary electrons emitted from the inserted stainless steel plate. Finally, $\sigma(E_e,v_r)$ was converted to $\sigma(E_e,E_c)$, functions of E_e and E_c, using the relation

$$E_c = \mu v_r{}^2/2 \quad (3)$$

where μ is the reduced mass of the system.

2-Bromothiophene (99%+) and 3-bromothiophene (99%+) were obtained commercially from Wako Pure Chemical Industries Ltd. They were used after several freeze−pump−thawed cycles. The sample was contained in a Pyrex tube outside the chamber during the experiments, and the Pyrex tube was connected with a steel tube inserted into the reaction cell in the chamber. The volatility of the sample at room temperature was high enough to create a sufficient concentration of target molecules in the gas phase, and the pressure was controlled at ca. 2×10^{-5} Torr.

III. Calculations

The geometrical parameters of the molecular 2BT and 3BT (C_4SBrH_3) were optimized using C_s symmetry, at the hybrid density functional B3LYP/6-311++G** level of theory. In the electron density contour maps obtained by Hartree−Fock self-consistent-field (HF−SCF) calculations with the 6-31+G(d) basis set, thick solid curves represent the repulsive molecular surfaces approximated by atomic spheres with van der Waals radii.[23] Ionization potential (IP) values calculated by outer valence Green's function (OVGF) method[24,25] and the third-order algebraic-diagrammatic construction (ADC(3)) scheme for the one-particle Green's function[24,26] were cited from ref 17 for assignments in the spectra.

As is well-known, the velocity dependence of the total scattering cross section of He*(2^3S) with He, Ar, and Kr has a very similar shape to that of Li(2^2S),[27] and interaction well-depths and the location of potential wells have been found to be very similar for interactions of various targets with He*-(2^3S) and Li(2^2S).[28−32] This similarity between He*(2^3S) and Li(2^2S) is usually exploited to compare the computationally more feasible target-Li potentials with the experimental results for the target-He*(2^3S) interactions.[2−7,13] In this work, the calculations of interaction potential with the Li(2^2S) atom, $V^*(R,\theta)$ (where R and θ are defined in the figure captions), were performed at the unrestricted second-order Møller−Plesset perturbation (UMP2) level of theory using the 6-31+G* basis set through scanning R or θ values, and the geometrical parameters of the targets were fixed at the previously optimized values. Spin-contamination was negligible for these calculations. The present calculations were performed with Gaussian 98.[33]

IV. Results

The He I UPS and He*(2^3S) PIES of 2BT and 3BT were shown in Figures 1 and 2, respectively. The energy scale for PIES was shifted 1.40 eV relative to that for UPS by the difference in the excitation energies between the He I photon (21.22 eV) and the He*(2^3S) (19.82 eV). The spectra in the higher IP (>17 eV) region were not shown because the very strong electron correlation leads to seriously overlapping bands.

The CERPIES for these two molecules were shown in Figures 3 and 4. Hot spectra at the higher collision energy ca. 250 meV were represented by dotted curves; cold spectra at the lower collision energy ca. 100 meV were represented by solid curves.

Log σ vs log E_c plots of CEDPICS in a collision energy range of 95∼300 meV were exhibited in Figures 5 and 6 for 2BT and 3BT, respectively. Electron density maps were also shown in the figures for grasping effective access directions of the He* atoms.

Figures 7−9 showed the calculated profiles of the interaction potential energies between the Li(2^2S) atom and the target molecule.

Tables 1 and 2 summarized orbital characters, the experimental and calculated IPs, experimental peak shifts (ΔE), and

TABLE 1: Band Assignment, Ionization Potentials (IP/eV), Peak Shifts (Δ*E*/meV), and Slope Parameters (*m*) for 2-Bromothiophene

band	orbital character	IP_{obsd}/ev	IP_{OVGF}/ev (pole strength)[a]	$IP_{ADC(3)}$/ev (pole strength)[b]	Δ*E*/meV	*m*
1	4a″ (π_3)	8.65	8.27(0.90)	8.53(0.89)	−70 ± 40	−0.30
2	3a″ (π_2)	9.50	9.22(0.90)	9.35(0.88)	−20 ± 20	−0.38
3	12a′ ($n_{Br}^{\parallel}$)	10.82	10.70(0.92)	10.67(0.91)	20 ± 0	−0.27
4	2a″ ($n_{Br}^{\perp}$)	11.37	11.23(0.90)	11.20(0.85)	−30 ± 0	−0.35
5	11a′ (n_S)	12.28	12.19(0.90)	12.30(0.89)	80 ± 60	−0.13
S1	(1a″*)[c]	(12.70)		12.44(0.16)		−0.30
6	10a′	13.33	13.20(0.90)	13.38(0.85)	(30 ± 40)	−0.28
7	1a″ (π_1)		13.18(0.83)	13.43(0.52)		
8	9a′	13.91	13.72(0.90)	13.97(0.88)		−0.15
9	8a′		13.85(0.89)	14.12(0.88)		
S2	(1a″)	(15.60)		15.70(0.10)		−0.29
10	7a′	16.41	16.66(0.86)	16.72(0.63)	30 ± 0	−0.08

[a] From ref 17. [b] From ref 17, only the selected satellites were given in this table. [c] * denoted as shake-up ($\pi_i^{-1}\pi_j^{-1}\pi_4^1$) involved band in ref 17.

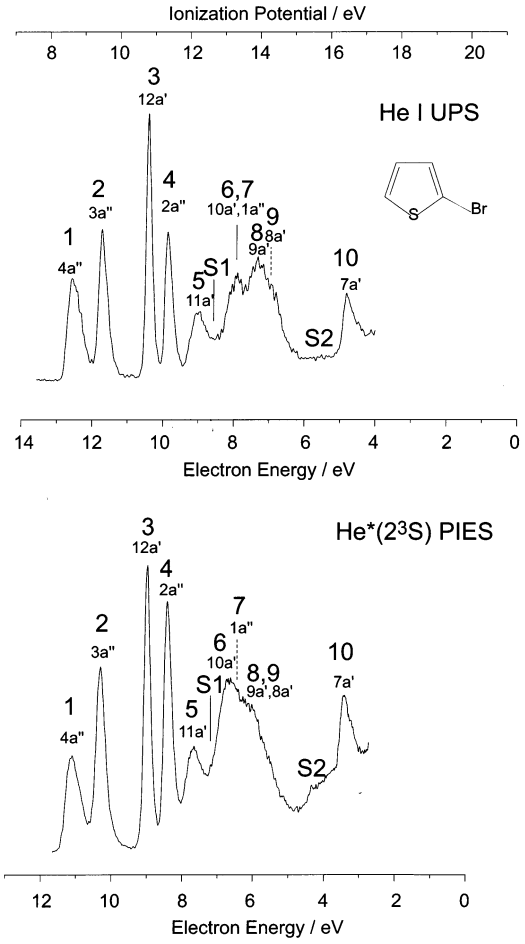

Figure 1. He I ultraviolet photoelectron spectrum and He*(2^3S) Penning ionization electron spectrum of 2-bromothiophene.

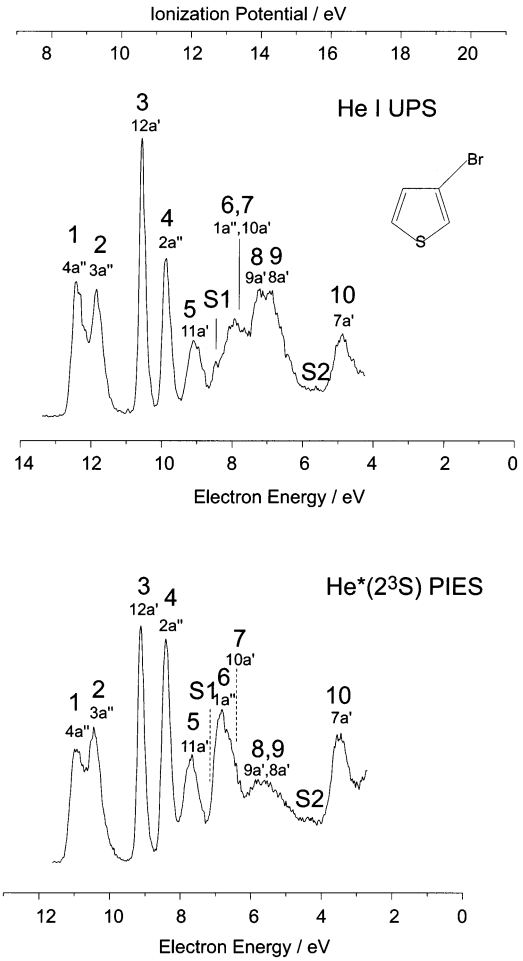

Figure 2. He I ultraviolet photoelectron spectrum and He*(2^3S) Penning ionization electron spectrum of 3-bromothiophene.

slope parameters (*m*) of CEDPICS. Only selected satellite states were assigned with the IPs, the details were represented in a separated figure which was reproduced by the ADC(3) results in ref 17. The *m* values were obtained by least-squares fitting the log σ vs log E_c plots. The experimental vertical IPs were determined by the present He I UPS. The Δ*E* values were obtained by ($E_{PIES} - E_{UPS} + 1.40$), where E_{PIES} and E_{UPS} were the peak position (in electron energy scale) in PIES and UPS, respectively.

V. Discussions

A. UPS and PIES of 2BT and 3BT. The He I UPS of monobromothiophenes (2BT and 3BT) were recorded in 1970s.[15,16] More recently, Potts et al. studied the valence shell photoelectron spectra of 2BT and 3BT both experimentally and theoretically, using synchrotron radiation as well as performing the ADC(3) calculations.[17] In that work, the details were presented for the main bands due to single-hole states and satellite bands due to the strong electron correlation effcts.[17] Because of the limitations of the energy range and energy resolution, only the ionization region of the outer valence orbitals and some specific satellites are discussed in this work.

At first sight, one can easily find the differences between the He I UPS in Figure 1 and that in Figure 2. The most obvious one concerns the IP difference between the ionic state of the highest occupied MO (HOMO) 4a″(π_3) orbital and the ionic

TABLE 2: Band Assignment, Ionization Potentials (IP/eV), Peak Shifts (Δ*E*/meV), and Slope Parameters (*m*) for 3-Bromothiophene

band	orbital character	IP_{obsd}/ev	IP_{OVGF}/ev (pole strength)[a]	$IP_{ADC(3)}$/ev (pole strength)[b]	Δ*E* /meV	*m*
1	4a″ (π_3)	8.80	8.48(0.90)	8.70(0.89)	-80 ± 40	−0.27
2	3a″ (π_2)	9.36	9.04(0.90)	9.21(0.88)	-10 ± 40	−0.36
3	12a′ ($n_{Br}^{\parallel}$)	10.63	10.52(0.92)	10.50(0.91)	-50 ± 10	−0.19
4	2a″ ($n_{Br}^{\perp}$)	11.33	11.21(0.90)	11.18(0.85)	-60 ± 0	−0.39
5	11a′ (n_S)	12.22	12.15(0.90)	12.24(0.89)	70 ± 0	−0.16
S1	(1a″*)[c]	(12.42)		12.73(0.27)		−0.37
6	1a″(π_1)	13.10	13.19(0.83)	13.26(0.21)		−0.23
7	10a′		13.15(0.90)	13.34(0.89)		
8	9a′	13.95	13.82(0.89)	14.02(0.86)		−0.11
9	8a′	14.32	14.09(0.89)	14.40(0.83)		
S2	(1a″)	(15.50)		15.18(0.11)		−0.38
10	7a′	16.35	16.46(0.87)	16.57(0.74)	20 ± 40	−0.03

[a] From ref 17. [b] Some satellite bands selected from ref 17 were given in this table. [c] * denoted as shake-up ($\pi_i^{-1}\pi_j^{-1}\pi_4^{1}$) involved band in ref 17.

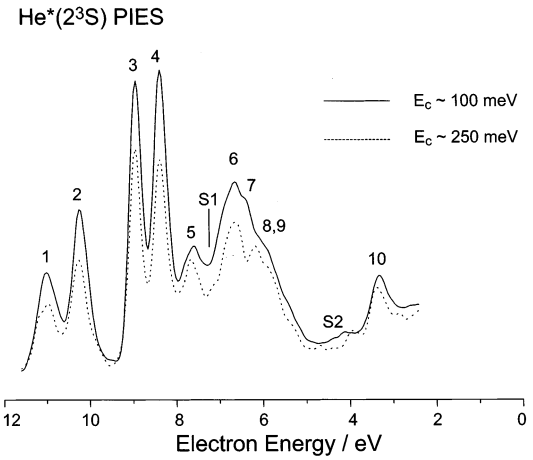

Figure 3. Collision-energy-resolved Penning ionization electron spectrum of 2-bromothiophene. Solid curve, $E_c = 98 \sim 102$ meV, average 100 meV; dotted curve, $E_c = 242 \sim 258$ meV, average 250 meV.

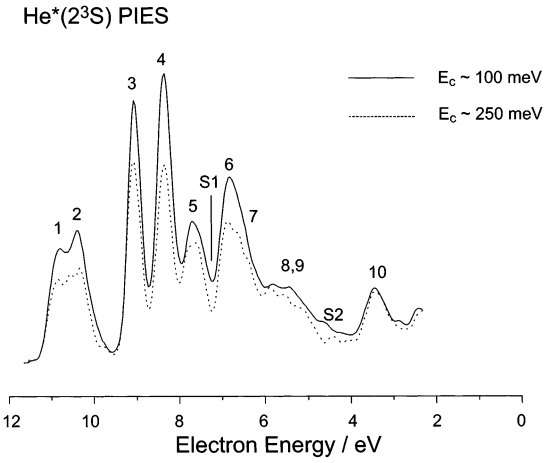

Figure 4. Collision-energy-resolved Penning ionization electron spectrum of 3-bromothiophene. Solid curve, $E_c = 97 \sim 103$ meV, average 100 meV; dotted curve, $E_c = 240 \sim 260$ meV, average 250 meV.

state of 3a″(π_2) orbital. The IP difference for 2BT, 0.85 eV, is larger than the value 0.56 eV for 3BT. This may be explained by different electron density distributions for these two orbitals of 2BT and 3BT. As shown in Figures 5 and 6, the almost collinear distribution of out-of-plane electrons is plotted for 4a″ of 2BT, whereas the triangle distribution is plotted for 4a″ of 3BT. Interactions among three parts separated by two nodal

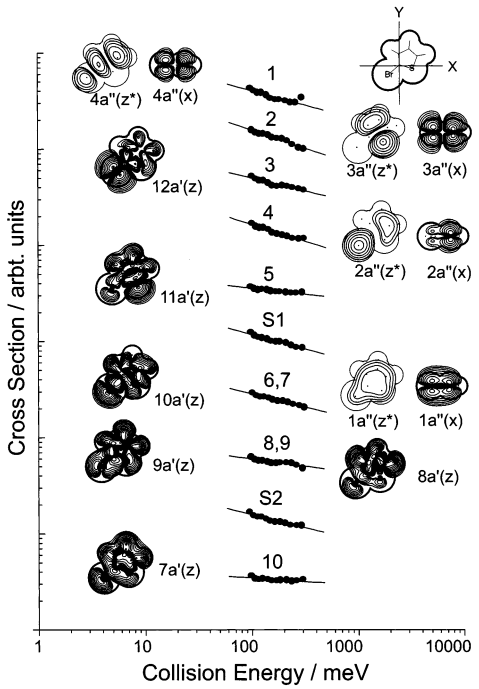

Figure 5. Collision energy dependence of partial ionization cross sections for 2-bromothiophene. The density maps noted with z were plotted on the molecular plane *XY*; those noted with z* were plotted on the plane above 1.7 Å (the van der Waals radium of carbon atom) from the molecular plane; those noted with x were plotted on the *YZ* plane.

planes for the former may be stronger than those for the latter, which further leads to the higher energy level of 4a″ for 2BT with respect to that for 3BT. Similarly, the effect of nodal planes causes the energy level of 3a″ for 3BT to be much higher than that for 2BT. It is more interesting to explore some band features in the PIES and UPS. First, band 2 (3a″, π_2) is slightly stronger than band 1 (4a″, π_3) in the UPS of 2BT, whereas the former is enhanced significantly in the PIES; the situation that band 1 is comparably strong as band 2 in the UPS holds in the PIES for 3BT. For 2BT, the exterior electrons of 3a″ are much more than those of 4a″, where the middle part of out-of-plane electron distributions for 4a″ is almost in the molecular surface (see Figure 5); for 3BT, the quantity of total exterior electrons summarized from three parts for 4a″ is comparable to that of 3a″ (see Figure 6). These distinct electron distributions are due to intramolecular orbital interactions, which will be discussed in the following text. Second, band 4 (2a″, the out-of-plane

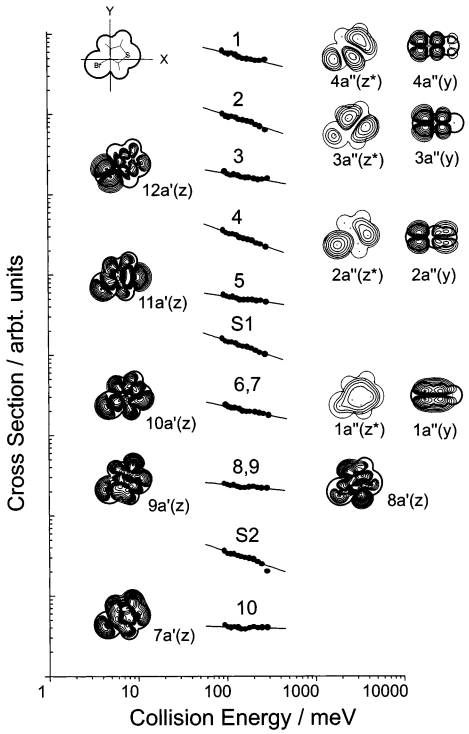

Figure 6. Collision energy dependence of partial ionization cross sections for 3-bromothiophene. The density maps noted with z were plotted on the molecular plane *XY*; those noted with z* were plotted on the plane above 1.7 Å (the van der Waals radium of carbon atom) from the molecular plane; those noted with y were plotted on the *XZ* plane.

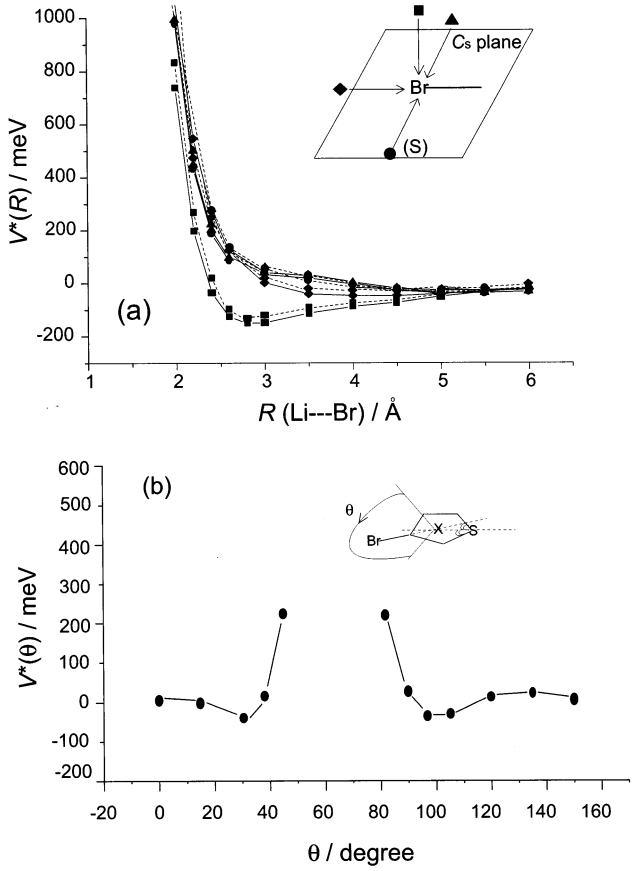

Figure 7. Interaction potential curves $V^*(R)$ for 2-bromothiophene − Li (solid lines) and 3-bromothiophene − Li (broken lines) in (a): (■), out-of-plane approach perpendicular to the C−Br bond axis; (▲), in-plane approach perpendicular to the C−Br bond axis (at the side far away from the sulfur atom); (●), in-plane approach perpendicular to the C−Br bond axis (at the side near the sulfur atom); (◆), access to the bromine atom along C−Br bond axis. Interaction potential curves $V^*(\theta)$ for 3-bromothiophene − Li in (b): scanning θ values in the molecular plane, X is the crossing point of the C−Br bond axis and the bisector of C−S−C angle.

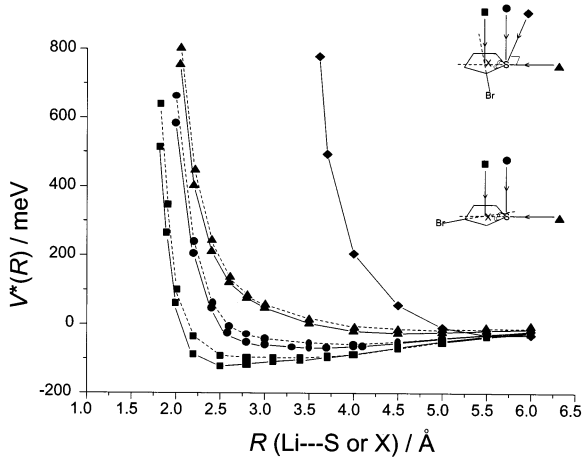

Figure 8. Interaction potential curves $V^*(R)$ for 2-bromothiophene − Li (solid lines) and 3-bromothiophene − Li (broken lines): (■), out-of-plane approach perpendicular to the thiophenyl plane and cross center X (X is defined in the caption of Figure 7); (▲), in-plane approach to the sulfur atom along the bisector of C−S−C angle; (●), out-of-plane approach to the sulfur atom; (◆), in-plane approach to the sulfur atom in the direction perpendicular to the bisector of C−S−C angle.

distribution of lone pair electrons of bromine atom $n_{Br}^{\perp}$) is weaker than band 3 (12a′, the in-plane distribution $n_{Br}^{\parallel}$) in the UPS for both 2BT and 3BT, but they are comparable in the PIES. Moreover, the intensity of band 6 (including ionization from 1a″, π_1 orbital) is enhanced in the PIES with respect to that in the UPS for both 2BT and 3BT. It is well-known that the π and n bands usually show relatively large enhancement of intensity in PIES because there are more electrons outside the molecular surface for these orbitals. They should exhibit relatively high reactivity in Penning ionization. In this work, the π_3, π_2 (especially π_2 orbital of 2BT), and n_{Br} orbitals are more reactive in Penning ionization. Actually, in the regions where the π or n electrons are distributed, the interactions are usually attractive, which will be discussed in section B. The enhancement of band 6 in the PIES with respect to the UPS concerns the satellite states, some arguments on the satellite states should be addressed below.

PIES has been known for strong enhancement of satellite bands due to a more complex ionization process than photon ionization.[34] Many satellites in the IP 12∼16 eV range are not resolved well in this work because of the low energy resolution. However, a satellite band S2 is still assigned for both 2BT and 3BT, it may correspond to one which has the highest IP value in Figure 10. On the basis of the analyses of CERPIES in Figures 3 and 4, another satellite band S1 may be recognized at the IP ca. 12.70 eV for 2BT or ca. 12.42 eV for 3BT. It corresponds to one satellite state (*) which has the lowest IP value in Figure 10. For band S1, a shake-up process in which excitation transition $\pi_i \rightarrow \pi_4$ ($i = 1, 2$) occurs (the π_4 is the lowest unoccupied MO (LUMO) 5a″)[17] should be involved in Penning ionization, whereas band S2 state corresponds to shake-off processes in which double-ionization occurs.[17] Because of the appearing sequence of main ionic states shown in Figure 10 and ref 17, the assignment of band 6 for 2BT differs slightly from that for 3BT. Thereby, the very steep shape at the lower

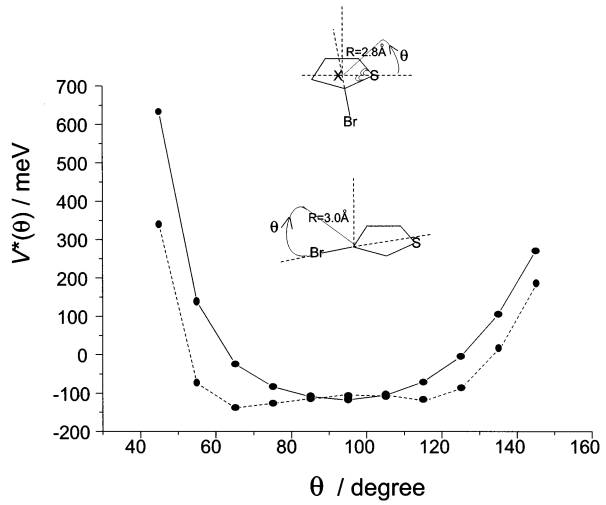

Figure 9. Interaction potential curves $V^*(\theta)$ for 2-bromothiophene − Li (solid lines) and 3-bromothiophene − Li (broken lines): scanning θ values in the plane perpendicular to the thiophenyl plane and cross the bisector of C−S−C angle for 2-bromothiophene; scanning θ values in the plane perpendicular to the thiophenyl plane and cross the C−Br bond axis for 3-bromothiophene.

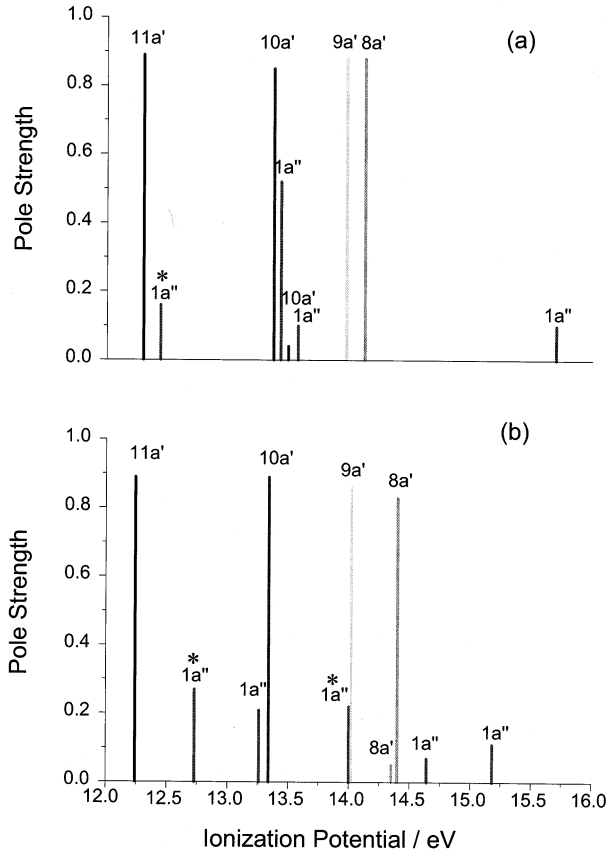

Figure 10. Ionization potentials and pole strength of ionic state (IP: 12.0 ∼ 16.0 eV) predicted by ADC(3) calculations (cited from ref 17). * shows the shake-up ($\pi_{1,2}$ to π_4) satellite states.

IP edge of band 6 for 3BT is due to the ionic sate of the 1a″ (π_1) orbital which appears prior to the 10a′ ionic state. The lower intensity of band 7 respective to that of band 6 for 3BT may suggest that there were not two (perhaps only one or no) satellite states of the 1a″ orbital in this IP range. It is contrast to the case of bands 6 and 7 for 2BT. Although the ADC(3) calculations did not predict the 1a″ satellite states occurring in this range,[17] these bands are very diffuse and overlapped and they exhibit higher intensities in the spectra of 2BT (see Figure 1).

B. Relative Reactivity of Orbitals with the He*(2^{3}S) Atom. The relative band intensities of PIES are closely related to the reactivity of the corresponding target MOs, further to the electrophilic reaction. On the other hand, CEDPICS reflects directly the reaction dynamics. The following part mainly focuses upon the slope parameters of CEDPICS for some specific bands and anisotropic interactions around the target molecules.

The first five bands correspond to ionic states for 4a″(π_3), 3a″(π_2), 12a′($n_{Br}^{\parallel}$), 2a″($n_{Br}^{\perp}$), and 11a′ (n_S, the in-plane distribution of lone pair electrons of sulfur atom) orbitals, where the orbital character is given by the main feature of the orbital electron composition. However, one can find that most of them show the mixed (or delocalized) electron compositions in electron density maps of Figures 5 and 6. Quantitative analysis of complex orbital composition dependent on substitution sites has been made in ref 17, where a typical case is the electron composition of the 3a″ orbital which is more complex for 3BT than that for 2BT. There are almost no contributions from the Br lone pair electrons for 3a″ orbital of 2BT.

The interactions between two reactants of Penning ionization have been investigated, based on the features of collision energy dependence of total ionization cross sections.[27,29,35] As discussed by Illenberger and Niehaus,[27] a simplified analytical expression for the repulsive part of the interaction potential, $\sigma(E_c) \propto \{\ln(B/E_c)\}^2(E_c/B)^{(b/d)-(1/2)}$, was given in the region of linear increase of the total cross sections $\sigma(E_c)$. This approximate expression implies the interaction potential in the entrance channel of Penning ionization $V^*(R) = B\exp(-dR)$ (R is the mutual distance). This model was successfully extended for CEDPICS analyses by Ohno et al.[36] When the minor dependence of $\{\ln(B/E_c)\}^2$ can be neglected, the slope parameter m is related to the parameters d and b by the equation $m = (b/d) - 1/2$.[36] b is the effective parameter of the transition probability $W(R) = C\exp(-bR)$ and determined by the lowest IP ($I(M)$) of the target molecule $b = 2\{2I(M)\}^{1/2}$. The anisotropic interactions can be reflected by the different m or d values. A very steep repulsive wall (hardcore) corresponding to a large d value results in a (b/d) smaller than $^1/_2$ and a negative slope parameter. When the long-range attractive term plays a dominated role, the m value is also negative $m = -2/s$ where s is the decay parameter of $V^*(R) = R^{-s}$.[36] However, the difference between the attractive and repulsive interactions can be recognized by the ΔE values. Typically, the positive ΔE value is often observed for the repulsive interactions. As shown in Tables 1 and 2 and Figures 5 and 6, the slope of band 8 for both 2BT and 3BT is almost flat over a positive peak shift, which indicates that the interaction around the σ_{CH} bond (orbital character of 7a′, to see Figures 5 and 6) should be repulsive. A positive peak shift ($\Delta E = 30 \pm 40$ meV) is observed for 10a′ of 2BT, although this band is seriously overlapped with band 7 and a negative slope is exhibited in Figure 5 for bands 6 and 7. As the orbital character of 10a′ is a σ_{CBr} bond, a repulsive interaction is expected for the He* approach along the bond axis (see Figure 7). We will pay more attention to the first five bands in the subsequent part. The slope parameters m for bands 2 ($m = -0.38$ for 2BT or -0.36 for 3BT) and 4 ($m = -0.35$ for 2BT or -0.39 for 3BT) are more negative than those for bands 1 ($m = -0.30$ for 2BT or -0.27 for 3BT) and 3 ($m = -0.27$ for 2BT or -0.19 for 3BT), respectively. The same sequence is observed for the peak shifts ΔE between bands 3 ($\Delta E = 20 \pm 0$ meV for 2BT or $\Delta E = -50 \pm 10$ meV for 3BT) and 4 ($\Delta E = -30 \pm 0$ meV for

2BT or $\Delta E = -60 \pm 0$ meV for 3BT), which is in contrast to the sequence between bands 1 ($\Delta E = -70 \pm 40$ meV for 2BT or $\Delta E = -80 \pm 40$ meV for 3BT) and 2 ($\Delta E = -20 \pm 20$ meV for 2BT or $\Delta E = -10 \pm 40$ meV for 3BT). The latter was also similarly observed for thiophene ($\Delta E = -150$ meV for the $\pi 3$ band or $\Delta E = 40$ meV for the $\pi 2$ band).[7] Generally, the sequences of the absolute m values for the first five bands are band 2 $\sim$ band 4 $>$ band 1 $\sim$ band 3 $\gg$ band 5 for 2BT and band 2 $\sim$ band 4 $>$ band 1 $\gg$ band 3 $\sim$ band 5 for 3BT. According to their orbital character assignments, we can derive such a conclusion that the He* approach perpendicular to the molecular plane (for the π and $n_{Br}^{\perp}$ orbitals) is more attractive than the in-plane approach (for 11a′, n_S). The calculated potentials for the model target-Li system are consistent with this conclusion. As shown in Figures 7 and 8, the in-plane approaches to the S and Br atoms in 2BT and 3BT exhibit the repulsive interactions, whereas the approaches perpendicular to the molecular plane including the S and Br atoms exhibit the attractive ones. The present UMP2/6-31+G* calculations predicted that there is a potential well with the depth of 160$\sim$140 meV for the He* approach to the thiophenyl center X defined in Figure 8, and a potential well with the depth of 170$\sim$180 meV occurs for the out-of-plane approach to the Br atom in Figure 7a. The in-plane sideways approach perpendicular to the C−Br bond axis is repulsive, which is similar to the monobromobenzene.[4] To reduce in-plane $n_{Br}-n_S$ interactions, the potential curve by scanning angle θ is shown only for 3BT in Figure 7b. Two potential wells (depth $\sim$ 50 meV) are located at certain positions slightly deviating from the line just perpendicular to the C−Br bond axis. This may be interpreted as $\pi-n$ bond interaction which results in changes of the angular distribution of the $n_{Br}^{\parallel}$ electrons. Moreover, a reasonable interpretation on the slope difference of CEDPICS for 12a′ orbitals of 2BT and 3BT will be given in section C.

To elucidate the interactions for the delocalized orbitals, the interaction potentials are scanned across the region where both aromatic π electrons and the perpendicular branch of the S lone pair electrons are distributed (to stimulate 3a″ orbital of 2BT) and the region where both the aromatic π and the $n_{Br}^{\perp}$ electrons are distributed (to stimulate 2a″ orbital of 3BT). As shown in Figure 9, a very wide potential well around the 3a″ orbital region means that this orbital should be very important for Penning ionization events. In fact, a very large negative slope parameter ($m = -0.38$) and a higher intensity respective to band 1 (4a″) are observed for band 2 (3a″) in the 2BT spectra. For the potential around the 2a″ orbital region, there are double minima: one is just above the Br atom; the other is in the π bond region. Details on intramolecular $\pi-n$ interaction as well as its effect on the anisotropic interaction will be presented in section C. The following part is to be concentrated on the π_1 band and its satellite bands.

Although the ionic state of π_1 orbital is seriously overlapped with the neighbor ionic state of 10a′ orbital, the slope parameter for a pure π_1 band is also estimated by the m values of bands S1, 6 and 7, and S2. The m value for the π_1 band of 2BT or 3BT may be $-0.30 \sim -0.35$. This value is very close to the experimental data for thiophene.[7] It indicates that the $n_{Br}^{\perp}$ and perpendicular branch of the S lone pair electrons interact weakly with the π_1 orbital and they are only the small contributions to the π_1 orbital. As discussed in section A, the shake-up (π_{1or2} to π_4) process is involved in the S1 state.[17] Ionization either from 1a″ (π_1), 2a″ (another configuration in this satellite state), or from the excited 5a″ (π_4) orbital exhibits a largely negative slope. Therefore, the slope parameter of band S1 is rather larger

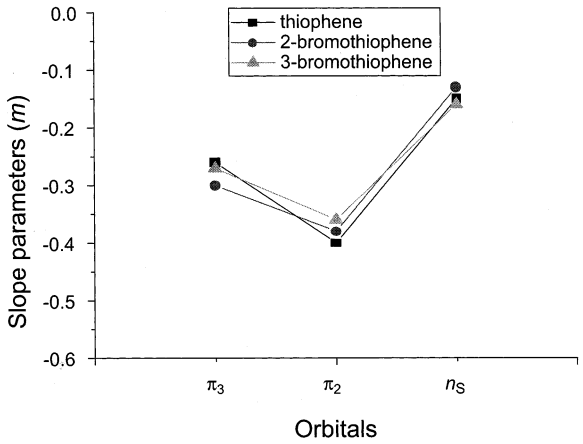

Figure 11. Slope parameters (m) of the π_2, π_3, and n_S orbitals for thiophene,[7] 2-bromothiophene, and 3-bromothiophene.

($m = -0.30$ for 2BT and -0.37 for 3BT). The slope for band S2 for 2BT is a little flatter than that for 3BT. It may be a result from the smaller configuration of the ionic state of the π_1 orbital for 2BT with respect to that for 3BT, which is in agreement with the ADC(3) predictions.[17]

C. Bromine Substitution Effect and Intramolecular Orbital Interaction. When we make comparison of the slope parameters of CEDPICS for the π orbitals of benzene and monobromobenzene,[4] the values are found to be scarcely changed. The same statement holds for thiophene[7] and monobromothiophenes. As shown in Figure 11, the slope parameters for the π_2, π_3, and n_S orbitals are correspondingly almost identical for thiophene, 2BT and 3BT. The reactivity of π orbitals of aromatic compounds would be expected to be unvaried when a halogen (Br) atom substitutes into them. However, the interactions around the Br atom substituted into molecules are anisotropic,[37] substitution sites may also affect upon the anisotropic reactivity with the He* atom.

The relative slope parameters of the $n_{Br}^{\parallel}$ and $n_{Br}^{\perp}$ bands with respect to the π_3 or π_2 band for the bromobenzene[4] and bromothiophenes are compared in Figure 12 parts a and b. The magnitude of the attractive interaction of the in-plane approach for $b_2(n_{Br}^{\parallel})$ is comparable with that of the out-of-plane approach for $b_1(n_{Br}^{\perp})$ for the bromobenzene, whereas the cases for the bromothiophenes are more complex. By symmetry, the $n_{Br}^{\perp}$ branch of the Br atom can interact with both π_3 and π_2 orbitals of the thiophene part; the $n_{Br}^{\parallel}$ branch of the Br atom can interact only with the lower lying σ orbitals of the thiophene part, especially with the n_S orbital. This will result in more complex orbital compositions for the bromothiophenes. Namely, the 2a″ orbital has some contributions of the π_3 and π_2 electrons, and the 12a′ orbital has some contributions of the n_S electrons. As the interactions are attractive for the π_3 and π_2 orbitals, the band of the mixed 2a″ orbital also exhibits an attractive interaction ($m = -0.35$ for 2BT and -0.39 for 3BT); the repulsive interaction for the n_S orbital leads to the less negative slope of CEDPICS for the 12a′ orbital ($m = -0.27$ for 2BT and -0.19 for 3BT). In particular, the substitution site effect also plays an important role because the slope of CEDPICS for the 12a′ orbital of 3BT becomes a little flatter with respect to a relatively negative one of 2BT. It may be explained by the following arguments. First, there is a larger n_S contribution in 3BT than in 2BT because of $n_{Br}^{\parallel}-n_S$ interactions. Second, for 3BT, there are a more widely repulsive region (near C−H bonds and S atom) and an attractive region for the $n_{Br}^{\parallel}$ which is shielded by the two neighboring repulsive areas of the C−H bonds, whereas for 2BT, the repulsive area of n_S is somewhat shielded by the

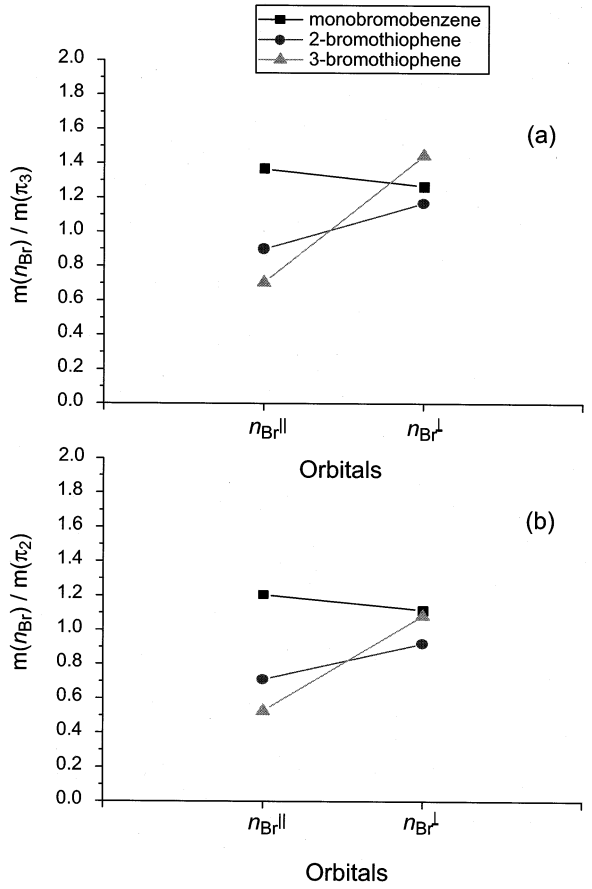

Figure 12. Relative slope parameters (m) of the $n_{Br}^{\parallel}$ and $n_{Br}^{\perp}$ orbitals respective to the π3 (a) and π2 orbitals (b) for monobromobenzene,[4] 2-bromothiophene, and 3-bromothiophene.

attractive area of the $n_{Br}^{\parallel}$. Thereby, the weak steric hindrance of the He* trajectory by the n_S electrons leads to the relatively negative slope of CEDPICS for the 12a′ orbital of 2BT.

VI. Conclusions

Monobromothiophenes (2BT and 3BT) are studied by two-dimensional Penning ionization electron spectroscopy as well as the model calculations of interaction potential energy for the 2BT(or 3BT)−He*(2^3S) system. Some satellite bands correlated with the ionic states of π orbitals are recognized by analyses of collision-energy resolved Penning ionization electron spectra. Approaches perpendicular to the thiophenyl plane including bromine atom are more attractive than the in-plane ones. The bromine substitution effect on the orbital reactivity is investigated through comparing the present results with the previous data of monobromobenzene[4] and thiophene.[7] We find that the reactivity of some orbitals of thiophene still holds for 2BT and 3BT in a sequence $\pi_2 > \pi_3 > n_S$. The intramolecular $n-\pi$ interactions for monobromothiophenes lead to the distinctly different slopes of CEDPICS for the lone pair n_{Br} orbitals of 2BT and 3BT. In particular, the bromine substitution in the 3 position reduces the magnitude of the attractive interaction of the in-plane approach for the $n_{Br}^{\parallel}$ orbital.

Acknowledgment. This work is partially supported by a Grant in Aid for Scientific Research from the Japanese Ministry of Education, Science and Culture. S.X.T. thanks the Japan Society for the Promotion of Science (JSPS) for a JSPS Research Fellowship (ID No. 00111).

References and Notes

(1) Ohno, K.; Yamakado, H.; Ogawa, T.; Yamata, T. *J. Chem. Phys.* **1996**, *105*, 7536.
(2) Kishimoto, N.; Aizawa, J.; Yamakado, H.; Ohno, K. *J. Phys. Chem. A* **1997**, *101*, 5038.
(3) Kishimoto, N.; Furuhashi, M.; Ohno, K. *J. Electron Spectrosc. Relat. Phenom.* **2000**, *113*, 35.
(4) Imura, K.; Kishimoto, N.; Ohno, K. *J. Phys. Chem. A* **2001**, *105*, 4189.
(5) Imura, K.; Kishimoto, N.; Ohno, K. *J. Phys. Chem. A* **2001**, *105*, 6073.
(6) Imura, K.; Kishimoto, N.; Ohno, K. *J. Phys. Chem. A* **2001**, *105*, 9111.
(7) Kishimoto, N.; Yamakado, H.; Ohno, K. *J. Phys. Chem.* **1996**, *100*, 8204.
(8) Hotop, H.; Niehaus, A. *Z. Phys.* **1969**, *228*, 68.
(9) Ohno, K.; Mutoh, H.; Harada, Y. *J. Am. Chem. Soc.* **1983**, *105*, 4555.
(10) Ohno, K.; Matsumoto, S.; Harada, Y. *J. Chem. Phys.* **1984**, *81*, 4447.
(11) Ohno, K.; Matsumoto, S.; Harada, Y. *J. Chem. Phys.* **1984**, *81*, 2183.
(12) Ohno, K.; Harada, Y. *Theoretical Models of Chemical Bonding*; Maksiæ, Z. B., Ed.; Springer-Verlag: Berlin, 1991; Part 3, p 199.
(13) Tian, S. X.; Chen, X. J.; Xu, C. K.; Xu, K. Z.; Yuan, L. F.; Yang, J. L. *J. Electron Spectrosc. Relt. Phenom.* **1999**, *105*, 99 and references therein.
(14) Heilbronner, E.; Maier, J. P. *Electron Spectroscopy: Theory, Techniques and Applications, Vol. 1.*; Brundle, C. R., Baker, A. D., Eds.; Academic Press: London, 1977.
(15) Rabalais, J. W.; Werme, L. O.; Bergmark, T.; Karlsson, L.; Siegbahn, K. *Int. J. Mass Spectrom. Ion. Phys.* **1972**, *9*, 185.
(16) Bozic, Z.; Humski, K.; Cvitas, T.; Klasinc, L. *J. Chem. Soc. Perkin Trans. 2* **1977**, *11*, 1413.
(17) Potts, A. W.; Trofimov, A. B.; Schirmer, J.; Holland, D. M. P.; Karlsson, L. *Chem. Phys.* **2001**, *271*, 337.
(18) Takami, T.; Ohno, K. *J. Chem. Phys.* **1992**, *96*, 6523.
(19) Mitsuke, K.; Takami, T.; Ohno, K. *J. Chem. Phys.* **1989**, *91*, 1618.
(20) Takami, T.; Mitsuke, K.; Ohno, K. *J. Chem. Phys.* **1991**, *95*, 918.
(21) Gardner, J. L.; Samson, J. A. R. *J. Electron Spectrosc. Relat. Phenom.* **1976**, *8*, 469.
(22) Kimura, K.; Katsumata, S.; Achiba, Y.; Yamazaki, T.; Iwata, S. *Handbook of He I Photoelectron Spectra of Fundamental Organic Molecules*; Japan Scientific: Tokyo, 1981.
(23) Pauling, L. *The Nature of the Chemical Bond*; Cornell University Press: Ithaca, New York, 1960.
(24) von Niessen, W.; Schirmer, J.; Cederbaum, L. S.; *Comput. Phys. Rep.* **1984**, *1*, 57.
(25) Zakrzewski, V. G.; Ortiz, J. V. *Int. J. Quantum Chem.* **1995**, *53*, 583.
(26) Schirmer, J.; Angonoa, G. *J. Chem. Phys.* **1989**, *91*, 1754.
(27) Illenberger, E.; Niehaus, A. *Z. Phys. B* **1975**, *20*, 33.
(28) Rothe, E. W.; Neynaber, R. H.; Trujillo, S. M. *J. Chem. Phys.* **1965**, *42*, 3310.
(29) Parr, T.; Parr, D. M.; Martin, R. M. *J. Chem. Phys.* **1982**, *76*, 316.
(30) Haberland, H.; Lee, Y. T.; Siska, P. E. *Adv. Chem. Phys.* **1981**, *45*, 487.
(31) Hotop, H. *Radiat. Res.* **1974**, *59*, 379.
(32) Hotop, H.; Roth, T. E.; Ruf, M.-W.; Yencha, A. J. *Theor. Chem. Acc.* **1998**, *100*, 36.
(33) Frisch, M. J.; Trucks, G. W.; Schlegel, H. B.; Scuseria, G. E.; Robb, M. A.; Cheeseman, J. R.; Zakrzewski, V. G.; Montgomery, J. A., Jr.; Stratmann, R. E.; Burant, J. C.; Dapprich, S.; Millam, J. M.; Daniels, A. D.; Kudin, K. N.; Strain, M. C.; Farkas, O.; Tomasi, J.; Barone, V.; Cossi, M.; Cammi, R.; Mennucci, B.; Pomelli, C.; Adamo, C.; Clifford, S.; Ochterski, J.; Petersson, G. A.; Ayala, P. Y.; Cui, Q.; Morokuma, K.; Malick, D. K.; Rabuck, A. D.; Raghavachari, K.; Foresman, J. B.; Cioslowski, J.; Ortiz, J. V.; Stefanov, B. B.; Liu, G.; Liashenko, A.; Piskorz, P.; Komaromi, I.; Gomperts, R.; Martin, R. L.; Fox, D. J.; Keith, T.; Al-Laham, M. A.; Peng, C. Y.; Nanayakkara, A.; Gonzalez, C.; Challacombe, M.; Gill, P. M. W.; Johnson, B. G.; Chen, W.; Wong, M. W.; Andres, J. L.; Head-Gordon, M.; Replogle, E. S.; Pople, J. A. *Gaussian 98*; Gaussian, Inc.: Pittsburgh, PA, 1998.
(34) Masuda, S.; Aoyama, M.; Ohno, K.; Harada, Y. *Phys. Rev. Lett.* **1990**, *65*, 3257.
(35) Niehaus, A. *Adv. Chem. Phys.* **1981**, *45*, 399.
(36) Ohno, K.; Takami, T.; Mitsuke, K.; Ishida, T. *J. Chem. Phys.* **1991**, *94*, 2675.
(37) Tian, S. X.; Kishimoto, N.; Ohno, K. *J. Electron Spectrosc. Relat. Phenom.* **2002**, in press.